RSC Advances

ROYAL SOCIETY OF CHEMISTRY

www.rsc.org/advances

Study of electronic and an enhanced thermoelectric (TE) properties of $Zr_xHf_{1-x-y}Ta_yNiSn$: A first principles study.

D. P. Rai[a,*], A. Shankar[c], Sandeep[b], M. P. Ghimire[c], R. Khenata[d] and R. K. Thapa[b,c]

Received Xth XXXXXXXXXX 20XX, Accepted Xth XXXXXXXXX 20XX
First published on the web Xth XXXXXXXXXX 200X
DOI: 10.1039/b000000x

A density functional theory (DFT) employing generalized gradient approximation (GGA) and modified Becke Johnson (TB-mBJ) potential have been used to study the electronic and thermoelectric (TE) properties of $Zr_xHf_{1-x-y}Ta_yNiSn$. The presence of indirect band gap at E_F in parent compound predict this material to be a small band gap insulator. The substitution of Ta atoms on the Hf site has inscreases the density of states (DOS) at E_F which facilitated the charge carrier mobility. The influence of Ta content has increased the Seebeck coefficient, electrical conductivity and suppress the thermal conductivity as a result the figure of merit ZT has enhanced. We have reported an increment of ZT value by 36% over undoped system. The theoretical data were compared with the experimental results.

1 Introduction

The Heusler compounds are the centre of scientific research since the time NiMnSb was predicted to be a half metal ferromagnet[1]. Due to its half metallic properties Heusler compounds are challenging in the field of spintronics[2–4]. Other than the half metallicity of Heusler compounds, it also has many interesting qualities such as high Curie temperature 730K for NiMnSb and 985 K for Co_2MnSi, the most stable zinc-blende structure[5], thermoelectric[6], etc. Among all other Heusler compounds, MNiSn (M=Ti, Hf, Zr) a type of half Heusler (HH) compound is of particular interest because of its narrow semi-conducting band gap[7]. Unlike other transition metal based HH compounds MNiSn (M=Hf, Zr) has no significant signature of high spin polarization (spin transport) at E_F. The chemical formula of HH alloys is XYZ, while X, Y, and Z can be selected from many different elemental groups (For example X= Ti, Zr, Hf, V, Mn, Nb; Y= Fe, Co, Ni, Pt; Z= Sn, Sb). The crystal structures of the ternary inter-metallic compounds were usually formed in the cubic MgAgAs type (space group F43 m)[8]. Some of these HH compounds with 18 valence electron counts per formula unit have narrow semiconducting band gap while metallic and sometimes magnetically ordered systems are found at both higher and lower electron counts[9]. This type of material is of great interest because of the large mobility of charge carriers as compared to other usual semi-conductors. This unique characteristic leads to a high Seebeck coefcient and moderate electric resistivity[10–12]. The higher value of Seebeck coefficient and low resisitivity is an evidence for these compounds to be a promising thermoelectric materials (TE-materials)[13–20,37]. In recent years, TE-materials have attracted much attention because it possesses all the qualities to be an alternative source for energy, which interplays an important role in energy conversion between heat and electricity. So far, several materials have been investigated to achieve the desired level of thermoelectric properties such as Heusler compounds, derivative of HH compound, Skutterudites, Zintl compound, $Ca_3Co_4O_9$, BiCuSeO[22–29]. However, the energy conversion efficiency of TE-materials are limited for commercial purposes. Highly efficient TE-materials are therefore an urgency. Thermoelectric efficiency is measured by a dimensionless figure of merit (ZT) which is in connection with the Seebeck coefficient (S), the electrical conductivity (σ) , the thermal conductivity (κ), and T is the absolute temperature. The ZT value around unity or more are considered to be good TE-material[30]. Typical TE-materials based on Tellurium, Lead, Antimony and Selenium with ZT values 0.85-1.20, considered to be more efficient, however they are not safe to handle due to its toxicity[31–33]. Therefore, searching for new low cost and environment friendly materials with high values of ZT pose a great challenge. Mostly studied thermoelectric properties for HH compounds were focused on the bulk materials[34–36]. An unannealed ZrNiSn shows ZT value around 0.64 at 800 K for undoped system[16]. The development of nano particle and thin film are advantageous for enhanced thermoelectric performance but they are very expensive computationally and experimentally. The thermoelectric efficiency was successfully enhanced in layered structure

[a] *Department of Physics, Pachhunga University College, Aizawl, India-796001.*
[b] *Department of Physics, Mizoram University, Aizawl,India-796009.*
[c] *Condensed Matter Physics Research Center, Butwal-13, Rupandehi, Lumbini, Nepal*
[d] *Laboratoire de Physique Quantique et de Modlisation Mathmatique (LPQ3M),Dpartement de Technologie, Universit de Mascara, 29000-Algeria*

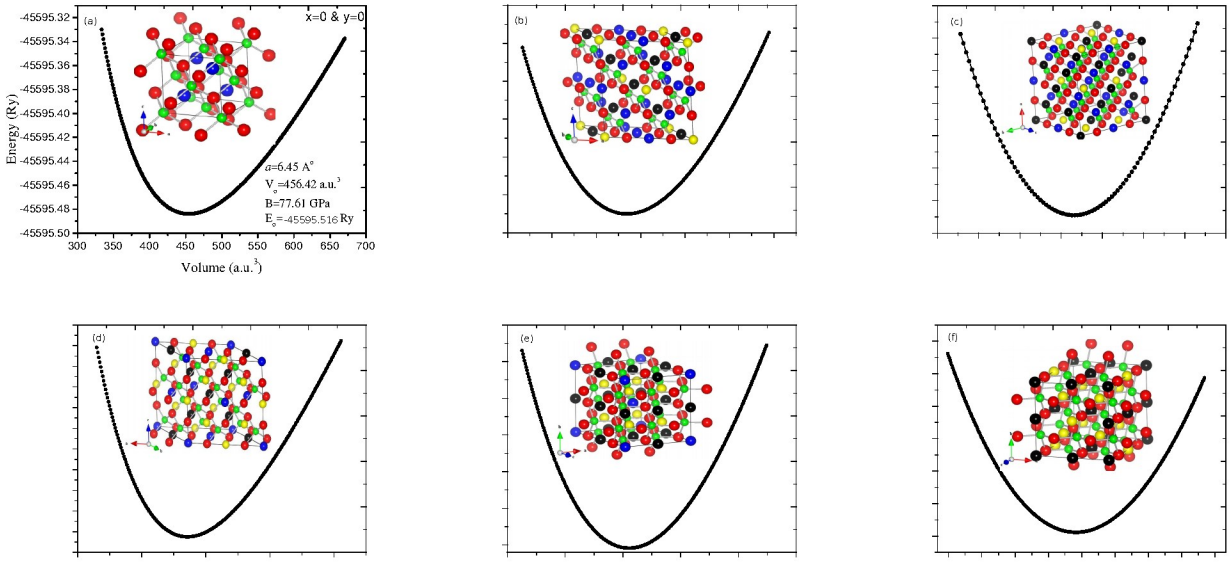

Fig. 1 Energy versus Volume and Crystal structure of $Zr_xHf_{1-x-y}Ta_yNiSn$ (a) x=0.00, y=0.00 (b) x=0.375, y=0.125 (c) x=0.375, y=0.250 (d) x=0.375, y=375 (e) x=0.375, y=0.500 and (f) x=0.375, y=0.625 (Hf-Blue, Ni-Red, Sn-Green, Zr-Black and Ta-Yellow)

BiCuOCh(Ch=S, Se and Te), Nano-structure, doping etc[37–39]. The room temperature power factor for nanosized TiNiSn[40] and thin film of HfNiSn[41] are 2.5 mW/mK^2 and 1.3 μW/K^2 cm respectively. Recently, band structure engineering is considered to be an effective method to improve ZT of bulk TE-materials. Thermoelectric properties of bulk semiconductors are in close relation with the electronic structure, which is sensitive to the stoichiometric composition. Yang *et al.* in their study have shown the relationship between the electronic structure and thermoelectric properties[42]. Similarly, the theoretical study conducted by Ye and his group using the first principle calculation have also come across the similar kind of relationship[43]. The doping of heavy elements in HH alloys have played a key role to reduce the thermal conductivity (κ) and band gap (E_g), attributes a dense energy bands near E_F, facilitates the electron transport and even induces half-metallicity in some cases[44–48]. The advancement of doping thallium impurity in PbTe results in an increased ZT value above 1.5 at 773 K[30]. Other than the conventional TE-materials a high value of ZT, 1.5 at 700 K has also been obtained in Ti doped HH $Ti_x(Zr_{0.5}Hf_{0.5})_{1-x}NiSn$[34]. The Bi-doped superlattice of ZrNiSn/$ZrNi_2Sn$ shows enhanced power factor of 3.3 mW/mK^2 as compared to 1.6 mW/mK^2 of Bi-doped bulk ZrNiSn[49]. This paper attempts to study the preparation of TE-material $Zr_xHf_{1-x-y}Ta_yNiSn$ with enhanced electrical conductivity and Seebeck coefficient by modifying the band energies near Fermi level with suitable doping. Optimized figure of merit ZT of $Zr_xHf_{1-x-y}Ta_yNiSn$ are enhanced with Ta doping.

2 Computational details

The electronic structures are calculated by adopting the full potential linearized augmented plane wave (FPLAPW) method for KS-DFT, as implemented in the WIEN2K package[50,53]. Two methods, GGA[51] and mBJ[52,53] are used to describe the electron exchange and correlation. Nonspherical contributions to the charge density and potential within the muffin tin (MT) spheres are considered up to $l_{max} = 10$ (the highest value of angular momentum functions). The cut-off parameter is R_{MT} x K_{max}=7 where K_{max} is the maximum value of the reciprocal lattice vector in the plane wave expansion and R_{MT} is the smallest atomic sphere radii of all atomic spheres. In the interstitial region the charge density and potential are expanded as a Fourier series with wave vectors up to G_{max}=12 a.u^{-1}. 286 special k points in the irreducible Brillouin zone are used for the selfconsistent DFT calculation. The convergence criteria for the selfconsistency is set to be 0.0001 Ry in the total energy. However the semicore states are treated semi-relativistically i.e. ignoring the spin-orbit(SO) coupling. The experimental lattice constants, 6.113 Å for ZrNiSn and 6.083 Å for HfNISn[8] were used for the ground-state structure optimization. The crystal structure of HH alloy MNiSn having space group $F43-m$ and atomic position M (1/4,1/4,14/) Ni(1/2,1/2,1/2) and Sn(0,0,0) were considered. The calculated

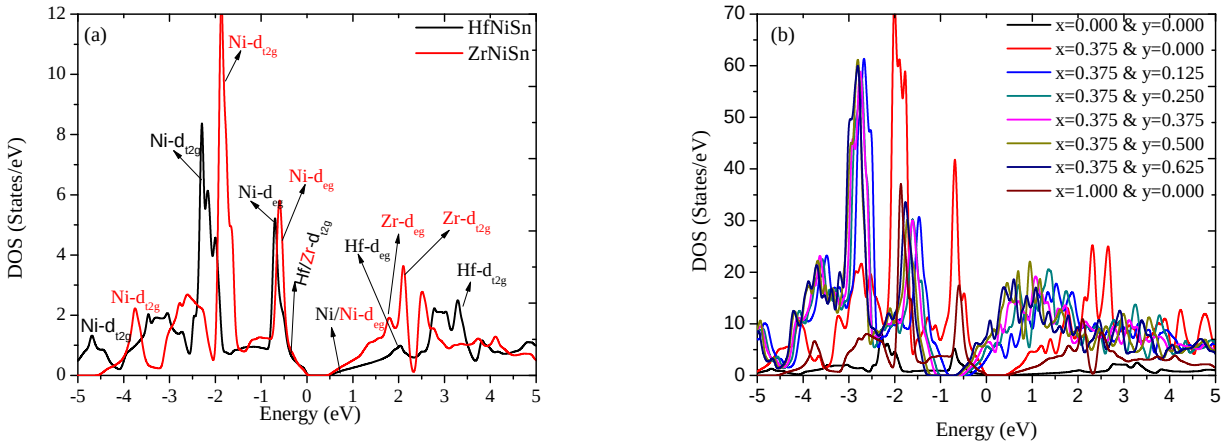

Fig. 2 Partial DOS of (a) HfNiSn/ZrNiSn (Black line represent HfNiSn and Red line ZrNiSn)and (b) Total DOS of $Zr_xHf_{1-x-y}Ta_yNiSn$

lattice constants are 6.45 Å for HfNiSn and 6.24 Å for ZrNiSn, larger than the available experimental data as usual for GGA. The crystal structures of $Zr_xHf_{1-x-y}Ta_yNiSn$ was constructed by a supercell method with 2x2x2 fcc cell along [1,1,1] direction and eight Ni/Hf atoms are generated. The composition $x = 0.375$ was generated by replacing three of the eight Hf atoms with three Zr atoms, as shown in Fig. 1. The crystal structures for the other compositions was constructed by replacing the remaining Hf atoms by Ta atoms as $y = 0.125$ (1/8), 0.250(2/8), 0.375(3/8), 0.500(4/8) and 0.625 (5/8). The relaxed structure for each of the composition was obtained from the total energy plot as a function of unit cell volume (Volume optimization)[57]. The crystal structures of each composition of $Zr_xHf_{1-x-y}Ta_yNiSn$ along with the volume optimization are presented in Fig. 1. Theoretically determined lattice constants for each of these $Zr_xHf_{1-x-y}Ta_yNiSn$ compounds are used for the calculation of electronic properties. For investigating the thermoelectric transport properties, we make use of the BoltzTraP[58] based on Boltzmann semiclassical theory with a 24x24x24 k-mesh inside the Brillouin zone. The Fermi energy at zero temperature ($T = 0$K) is taken as the chemical potential in the transport calculation.

3 Results and discussions

In order to examine the alloying stability of $Zr_xHf_{1-x-y}Ta_yNiSn$ structures (at 0 K), we have calculated the energy of formation (ΔE_f). The formation energy gives an idea about the existence of stable crystal. Furthermore, the negative values of ΔE_f indicates stronger bonidng between the atoms and more alloying stability of the crystal[54]. The energy of formation (ΔE_f) of a compound $Hf_xNi_ySn_z$ (say) is calculated by subtracting the sum of the energies (xE_{Hf}+yE_{Ni}+zE_{Sn}) of pure constituent elements in their stable crystal structures from the total energy (E_f) of the compound. Therefore, the ΔE_f of the compound $Hf_xNi_ySn_z$ is calculated using the following expression[55,56]:

$$\Delta E_f = \frac{E_f - (xE_{Hf} + yE_{Ni} + zE_{Sn})}{(x+y+z)} \quad (1)$$

Here, E_f is the total energy of the compound, E_{Hf}, E_{Ni} and E_{Sn} denotes the total energy per atom of the pure element Hf, Ni and Sn where x, y, z are the number of Hf, Ni and Sn atoms in the primitive cell respectively. The calculated total energy, formation energy and the individual energies of the constituent atoms are presented in Table 1

3.1 Electronic properties

For calculating the electronic structure, the optimal lattice constants were used. The previous report revealed that Hf/ZrNiSn are semiconductors with an indirect band gap of ~ 0.50 eV[6,7,13,59]. Our results are in good agreement with the indirect band gap between Γ-X points in the Brillouin Zone as shown in Figs. 3 (a, b). The band gap is mainly formed by the hybridization of M(d-e_g, d-t_{2g}) and Sn-p orbitals with some Ni (d-t_{2g}) orbitals as shown in Figs.2(a, b). As shown in Fig. 3(a, b) the top of the valence band (M-d-t_{2g}) degenerate into three sub-bands along Γ point, the two with heavier masses are at lower energy (below -2.0 eV). Mean while the lowest conduction band is formed by Ni (d-e_g) and are non-degenerated. In most cases LDA/GGA band gaps are underestimated[49,60]. Whereas in case of HH MNiSn the theoretical band gaps overestimated the experimental values obtained from resisitivity measurements (E_g=0.18 ev for Zr and

Table 1 The total number of atoms (n) in a compound, total energy (E_f in Ry) of the compound, total energy of the individual atoms E_M(M=Hf,Ni,Sn,Zr,Ta) in Ry, formation energy (ΔE_f in Ry) and the formation energy per unit cell (ΔH_f in Ry/a.u.^{3})

Compound	n	E_f (Ry)	E_{Hf}(Ry)	E_{Ni}(Ry)	E_{Sn}(Ry)	E_{Zr}(Ry)	E_{Ta}(Ry)	ΔE_f(Ry)	ΔH_f (Ry/a.u.^{3})
$Hf_1Ni_1Sn_1$	3	-45595.516	-7949.873	-801.581	-3281.838	0.000	0.000	-11187.408	-99.898
$Zr_3Hf_4Ta_1Ni_8Sn_8$	24	-296830.385	-7949.873	-801.581	-3281.838	-1910.277	-8228.033	-9100.195	-94.697
$Zr_3Hf_3Ta_2Ni_8Sn_8$	24	-297885.921	-7949.873	-801.581	-3281.838	-1910.277	-8228.033	-9132.585	-96.110
$Zr_3Hf_2Ta_3Ni_8Sn_8$	24	-298945.624	-7949.873	-801.581	-3281.838	-1910.277	-8228.033	-9165.149	-89.621
$Zr_3Hf_1Ta_4Ni_8Sn_8$	24	-299998.754	-7949.873	-801.581	-3281.838	-1910.277	-8228.033	-9197.441	-99.280
$Zr_3Hf_0Ta_5Ni_8Sn_8$	24	-301388.321	0.000	-801.581	-3281.838	-1910.277	-8228.033	-9243.749	-95.834
$Zr_1Ni_1Sn_1$	3	-22598.345	0.000	-801.581	-3281.838	0.000	0.000	-5534.883	-50.218

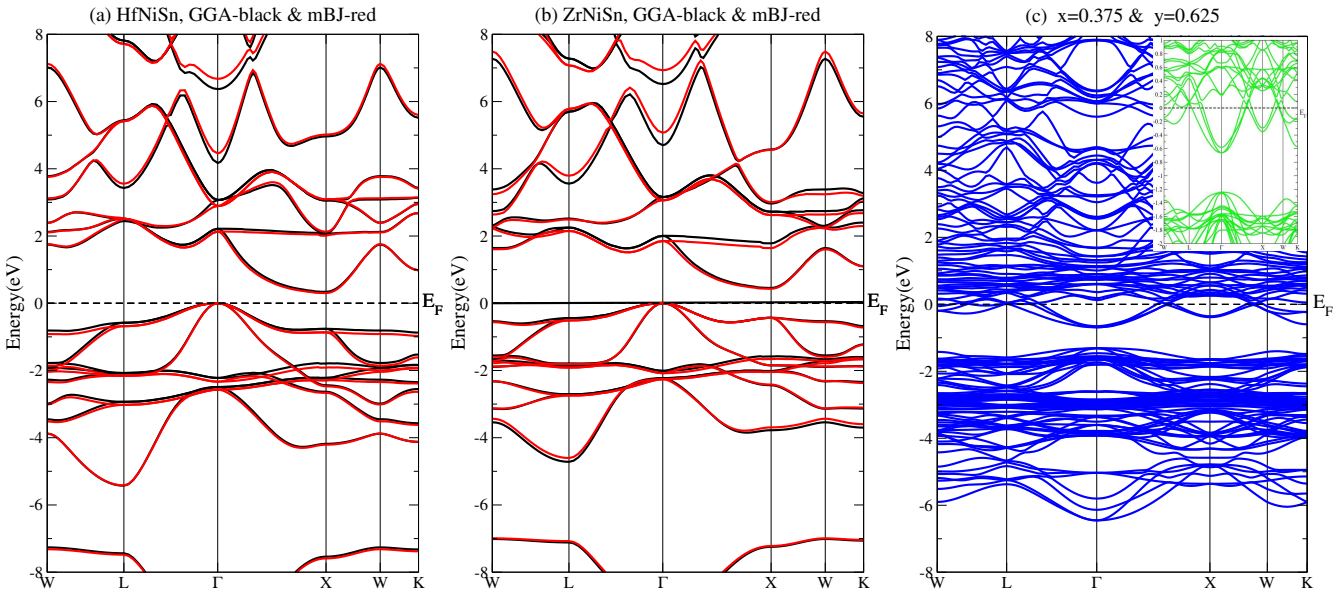

Fig. 3 Band structures of (a) HfNiSn, (b) ZrNiSn and (c) $Zr_xHf_{1-x-y}Ta_yNiSn$ (x=0.375, y=0.625)

0.18 eV for Hf)[6,7,13,59]. Our calculation of electronic structure with modified Becke Johnson (mBJ)[52,53] is almost ineffective as there is no improvement in the band gap [see 3(a,b)]. Do *et al.*[49] have reported that even an implementation of highly sophisticated hybrid functional proposed by Heyd-Scuseria-Enzerhof (HSE06)[61] shows a negligible effect on its band gap. Thus we employed a computationally cheap exchange correlation (GGA) to treat these kind of systems. On the other hand the doping of Ta atoms has shifted the band gap towards the lower energy as a result the Ni-d states disperse around the E_F and the metallic character predominates (Fig.2c), similar behaviour was reported in (Zr, Hf)$Ni_{1+x}Sn$ with increasing Ni dopants[20]. With Ta doping the systems are metallic and hence non-local effects are not considered. Hence, all the systems with increasing doping concentrations are treated within GGA.

3.2 Thermoelectric properties

In this section the temperature dependent Seebeck coefficient S, thermal conductivity κ, electrical conductivity divided by the scattering time σ/τ are calculated from the semiclassical transport equation as implemented in computational code called BoltzTrap[58]. Equation 1 interprets electrical conductivitiy tensors[62]:

$$\sigma_{\alpha,\beta} = e^2 \Sigma_{i,k} \left[-\frac{\partial f_0(T,\varepsilon,\mu)}{\partial \varepsilon} \right] v_\alpha v_\beta \tau_k \qquad (2)$$

where α, β are the tensor indices, v_α and v_β are the group velocities, e is the electron charge and τ_k is the relaxation time. The electrons contribution remain near the chemical potential (μ) in a narrow range of $\mu - k_B T < \varepsilon < \mu + k_B T$, where k_B is the Boltzmann constant[63]. The transport distribution is written as[64]

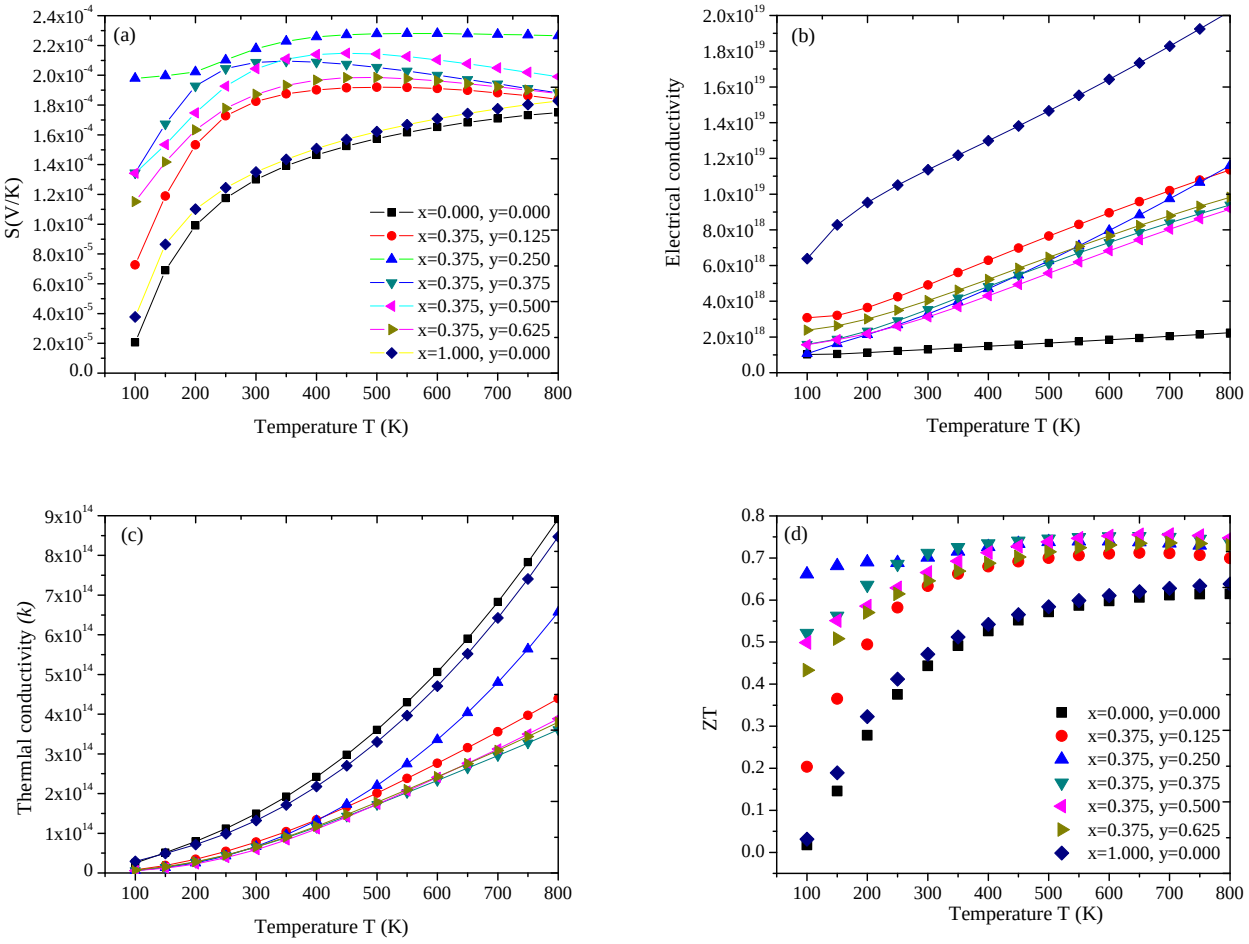

Fig. 4 (a)Seebeck coefficient S (V/K), (b) Electrical conductivity σ/τ $(\Omega ms)^{-1}$,(c) Thermal conductivity k (W/mKs) and (d) ZT of $Zr_xHf_{1-x-y}Ta_yNiSn$

$$\Xi_{i,k} = \Sigma_{i,k} v_\alpha v_\beta \tau_k \tag{3}$$

which is the kernel of all transport coefficients. From the rigid band approach, the electrical conductivity, thermal conductivity and Seebeck coefficient can be written as a function of temperature (T) and chemical potential (μ) by integrating the transport distribution [65]

$$\sigma = e^2 \int \Xi_{i,k} \left[-\frac{\partial f_0(T,\varepsilon,\mu)}{\partial \varepsilon} \right] d\varepsilon \tag{4}$$

$$\kappa = k_B^2 T \int \Xi_{i,k} \left(\frac{\varepsilon - \mu}{k_B T} \right)^2 \left[-\frac{\partial f_0(T,\varepsilon,\mu)}{\partial \varepsilon} \right] d\varepsilon \tag{5}$$

$$S = \frac{e k_B}{\sigma} \int \Xi_{i,k} \left(\frac{\varepsilon - \mu}{k_B T} \right) \left[-\frac{\partial f_0(T,\varepsilon,\mu)}{\partial \varepsilon} \right] d\varepsilon \tag{6}$$

Here f_0 is a Fermi-Dirac distribution function.The thermoelectric efficiency of TE-materials are in close relation with the electronic band structure and the thermal conductivity. The code BoltzTraP include only the electronic thermal conductivity (κ) whereas the phonon contribution is neglected. The Seebeck coefficient is a sensitive test of the electronic structure at the vicinity of the E_F. Thus it can be increased by increasing the DOS (in relation with effective mass) near edge E_F by doping heavy elements (see Fig.3(c)). The charge transport are due to the two narrow bands along Γ symmetry near E_F between M-d_{t2g} and Ni-d_{eg}. The lower bands at -1.3 eV (M-d_{t2g}) are more flat as compared to the upper bands at -0.6 eV (Ni-d_{eg}), see Fig. 3c (inset). The dense bands near E_F facilitated the transport of charge carriers [62]. The chemical potential is equivalent to Fermi energy at $T = 0$ K.

The thermoelectric efficiency denoted as ZT (figure of

Table 2 Comparison of figure of merit ZT of $Zr_xHf_{1-x-y}Ta_yNiSn$ with the experimental data

Present calculation (750 K)				Previous experimental data			
x	y	S ($\mu V/K$)	ZT	x	y	ZT	References
0.000	0.000	165	0.55	0.00	0.000	0.42 (800 K)	[37]
0.375	0.125	185	0.68	0.30	0.010	0.70 (870 K)	[66]
0.375	0.250	230	0.70	0.25	0.060	0.30 (790 K)	[68]
0.375	0.375	190	0.75	0.35	0.020	0.50 (875 K)	[46]
0.375	0.500	200	0.75	0.50	0.010	1.00 (873 K)	[19]
0.375	0.625	195	0.73				
1.000	0.000	170	0.52	1.00	0.000	0.64 (800K)	[16]
				0.40	0.020	0.70 (880 K)	[19]
				0.30	0.050	0.85 (870 K)	[66]
				0.30	0.000	0.30 (870 K)	[66]

merit) has been calculated from equation (7).

$$ZT = \frac{S^2\sigma T}{\kappa} \tag{7}$$

The high value of ZT is related with high value of S and low value of κ. The $ZT \sim 1$ is considered to be a benchmark value for the practical application of TE-materials[30]. Subsequently, the thermoelectric properties of the systems were investigated in the range $(50-800)K$. The calculated S, σ/τ, κ and ZT are presented in Fig. 4. In our case we have achieved a dense band near E_F as compared to undoped system by doping Ta atoms as shown in Fig.3(a-c). In Fig. 4(a), we have seen the increasing magnitudes of S with increasing doping concentration at all temperatures, indicating the more carrier concentrations. Our plot of S shows the similiar behaviour as that of experimetal plot (see Fig. 4a)[66]. The absolute value of S increases above $200\mu V/K$ (x=0.375, y=0.250, 0.375 and 0.50) at 400 K and remains almost constant upto 650 K (see Table 2). The S values for the samples with compositions $Zr_{0.25}Hf_{0.25}Ti_{0.5}NiSn$[67] agree well with these results. In Fig. 4b, the electrical conductivity(σ/τ) is seen to increase over the whole temperature range, showing semiconducting like behaviour. The values are comparable to resistivity curve as it is just the inverse of (σ/τ) which means the resistivity decreases with the increase in temperature as those reported for $Zr_{0.30}Hf_{0.70}Ta_{0.05}NiSn$ (see Fig. 3a)[66]. In our calculation the σ/τ is highest for the undoped system (x=0.0, y=0.0) as the doping concentration increases, the value decreases. The evolution of the thermal conductivity κ is plotted in Fig. 4(c). It shows that κ is linearly dependent on temperature (T), which shows similar behaviour as that of experimental plot (see Fig. 4c)[66]. The calculated κ value is highest for the undoped system which agrees well with the experimental results[66].The dimensionless figure of merit ZT is calculated from the measured physical properties by using the equation 7 and is presented in Fig. 4(d). ZT reaches maximum values between 0.70-0.75 in the temperature range from 300 K to 800 K which are in qualitative agreement with the experimental results[19,46,66,68]. At higher temperatures the value slightly decreases, due to a decrease in S and sharp increase in κ. The calculated ZT values and Seebeck coefficient (S) at 750 K for all compositions together with the experimental results are shown in Table 2.

4 Conclusion

In most of the studied cases,the half Heusler (HH) compounds with exactly 18 valence electrons does not show spin polarization at E_F unlike other Heusler compounds, they are semiconductors/semi-metals. The compound MNiSn(M=Hf, Zr) under our investigation with exact counts of 18 valence electrons shows semiconduting behaviour with a small band gap of around $\sim$0.50 eV. The character of optimized thermoelectric property is possible in $Zr_xHf_{1-x-y}Ta_yNiSn$ with enhanced efficiency. Unfortunately, our system could not achieve the benchmark value i.e. 1 for its commercial application. The maximum calculated ZT is 0.75 at 750 K. Though we could not mimic the exact experimental composition but the results follow the similar trend and it is in good agreement with the previous experimental result of 0.85 at 870 K. In our case the ZT value for the doped system is enhanced by 36% over the undoped sample ($ZT = 0.55$). However higher values of ZT are expected if the S and κ are improved. For future work, all those related parameters can be optimized to enhance the ZT above unity by means of suitable doping of the heavy atoms and improving the density of states near E_F. Further, some other theoretical techniques(thin film or nano

structure) may be opted for the improvement of *ZT* within a suitable temperature range.

Acknowledgment

DPR acknowledges research fellowship from Beijing Computational Science Research Center (Beijing, China). AS and RKT a research grant from UGC (New Delhi, India). MPG acknowleges the partial support from NIMS, Japan. SD a grant from DST,New Delhi, India under Dy No. SERB/F/3586/2013-14 dated 6.09.2013.

References

1 R. A. de Groot, F. M. Mueller, P. G. van Engen and K. H. J. Buschow, *Phys. Rev. Lett.* 1983, **50** 2024.

2 S. Ishida, S. Fujii, S. Kashiwagi and S. Asano, *J. Phys. Soc. Jpn.* 1995, **64** 2152.

3 A. Sadoc, C. de Graaf and R. Broer, *Phys. Rev. B* 2007, **75**, 165116

4 A. Fert, *Rev. Mod. Phys.* 2008, **80**, 1517.

5 P.J. Webster and K. R. a Ziebeck,*Alloys and Compounds of d-elements with Main Group Elements. Part2 edited by H. R. J Wijn, Landolt-Bornstein, New series Group III Vol. 32/c* Springer Berlin 64-414 2001.

6 F. G. Aliev, *Physica B* 1991, **171**, 199.

7 S. Ogut, K.M. Rabe, *Phys. Rev. B* 1995, **51**, 10443.

8 W. Jeitschko, Metall. Trans. A 1 , 3159 (1970).

9 L. Offernes, P. Ravindran, A. Kjekshus, *J. Alloys Compd.* 2007, **439** 2007, 37.

10 C. Uher, J. Yang, S. Hu, D.T. Morelli, G.P. Meisner, *Phys. Rev. B* 1999, **59**, 8615.

11 H. Hohl, A.P. Ramirez, C. Goldmann, G. Ernst, B. Wolng, E. Bucher, *J. Phys. Condens. Matter* 1999, **11**, 1697.

12 S. Bhattacharya, A.L. Pope, R.T. Littleton IV, T.M. Tritt, V. Ponnambalam, Y. Xia, S.J. Poon, *Appl. Phys. Lett.* 2000, **77**, 2476.

13 P. Larson, S. D. Mahanti, and M. G. Kanatzidis, *Phys. Rev. B* 2000, **62**, 12754.

14 Q. Shen, L. Zhang, L. Chen, T. Goto, and T. Hirai, *J. Mater. Sci. Lett.* 2001, **20**, 2197-2199.

15 J. D. Germond, P. J. Schilling, N. J. Takas, and P. F. P. Poudeu, *MRS Proc.* 2010, **1267**, 2010.

16 P. Qiu, J. Yang, X. Huang, X. , and L. Chen, *Appl. Phys. Lett.* 2010, **96**, 152105.

17 Y. Kimura, T. Tanoguchi, Y. Sakai, Y.-W. Chai, and Y. Mishima, *MRS Proc.* 2011, **1295**.

18 M.-S. Lee and S. D. Mahanti, *Phys. Rev. B* 2012, **85**, 165149.

19 S. Chen, K. C. Lukas, W. Liu, C. P. Opeil, G. Chen, and Z. Ren, *Adv. Energy Mater.* 2013, **3**, 12101214.

20 V. Romaka, P. Rogl, L. Romaka, Y. Stadnyk, A. Grytsiv, O. Lakh, and V. Krayovskii, *Intermetallics* 2013, **35**, 45.

21 D. F. Zou, S. H. Xie, Y. Y. Liu, J. G. Lin, and J. Y. Li, *J. Appl. Phys.* 2013, **113**, 193705.

22 J. Schmit, Z. M. Gibbs, G. J. Snyder and C. Felser *Mater. Horiz.* 2015 **2** 68-75.

23 C. Fu, T. Zhu, Y. Liu, H. Xie and Zhao *Energy Environ.Sci* 2015 **8** 216-220.

24 R. A. Downie, D. A. MacLaren, R. I. Smith and J. W. G. Bos *Chem. Commun* 2013 **49** 4184-4186.

25 D. K. Misra, A. Bhardwaj and S. Singh *J. Mater. Chem. A* 2014 **2**11913-11921.

26 M. K. Bravo, A Moure, J. F. Fernandez and M. M. Gonzalez *RSC Adv.* 2015 **5** 41653-41667.

27 Q. Shi, Z. Feng, Y. Yan and Y. X. Wang *RSC Adv.* 2015 **5** 65133-65138.

28 T. Wu, T. A. Tyson, J. Bai, K. Pandya, C. Jaye and D. Fischer *J. Mater. Chem. C* 2013 **1** 41214-41221.

29 L. D. Zhao, J. He, D. Berardan, Y. Lin, J. F. Li, C. W. Nan and N. Dragoe *Energy Environ. Sci.* 2014 **7** 2900-2924.

30 J. P. Heremans, V. Jovovic, E. S. Toberer, A. Saramat, K. Kurosaki, A. Charoenphakdee, S. Yamanaka and G. J. Snyder, *Science* 2008, **321**, 554.

31 G. E. Smith and R. Wolfe, *J. Appl Phys.* 1962, **33**, 841.

32 D. Y. Chung, T. Hogan, J. Schindler, L. Iordarridis, P. Brazis, C. R. Kannewurf, C. Baoxing, and C. Uher, *Complex bismuth Chalcogenides as thermoelectrics* Proceedings XVI ICT 5-8, May,Cat. No.97TH8291, 1997.

33 M. Bala, S. Gupta, T. S. Tripathi, S. Verma, S. K. Tripathi, K. Asokan and D. K. Avasthi *RSC Adv.* 2015 **5** 25887-25895.

34 N. Shutoh and S. Sakurada, *J. Alloys Compd.* 2005, **389**, 204.

35 S.-W. Kim, Y. Kimura, Y. Mishima, *Intermetallics* 2007, **15**, 349.

36 S. Katsuyama, R. Matsuo, M. Ito, *J. Alloys Compd.* 2007, **428**, 262.

37 D. Zou, S. Xie, Y. Liu, J. Lin and J. Li *J. Mater. Chem. A* 2013 **1** 8888-8896.

38 P. Jood, R. J. Mehta, Y. Zhang, T. B. Tasiuc, S. X. Dou, D. J. Sing and g. Ramanath *RSC Adv.* 2014 **4** 6363-6368.

39 M. U. Kahalay and U. Schwingenschlogl *J. Mater. Chem. A* 2014 **2** 10379-10383.

40 Y. W. Chai and Y. Kimura, *Appl. Phys. Lett.* 2012, **100**, 033114.

41 S. -H Wang, H. -M. Cheng , R. -J. Wu, and W. -H. Chao, *Solid Thin Films* 2010, **518**, 59015904.

42 G. Yang, Y. Yang, Y. Yan and Y. Wang *Phys. Chem. Chem. Phys.* 2014 **16** 5661-5666.

43 L. Ye, Y. X. Wang, J. Yang, Y. Yan, J. Zhang, L. Guo and

Z. Feng *RSC Adv.* 2015 **5** 50720-50728.

44 H. Hazama, M. Matsubara, R. Asahi, T. Takeuchi, *J.Appl. Phys.* 2011, **110**, 063710.

45 K. Miyamoto, A. Kimura, Kazuaki Sakamoto, M. Ye,Y. Cui, K. Shimada, H. Namatame, M. Taniguchi, S. Fujimori, Y. Saitoh, E. Ikenaga, K. Kobayashi, J. Tadano, T. Kanomata, *Appl. Phys. Express* 2008, **1**, 081901.

46 H.H. Xie, J.L. Mi, L. Peng. Hu, N. Lock, M. Christensen, C.G. Fu, B.B. Iversen, X.B. Zhao, T.J. Zhu, *Cryst EngComm* 2012, **14**, 4467.

47 Z. Zhu, Y. Cheng, U. Schwingenschlogl, *Phys. Rev.B* 2011, **84**, 113201.

48 S. R. Culp, S. J. Poon, N. Hickman, T. M. Tritt and J. Blumm, *Appl. Phys. Lett.* 2006, **88**, 042106.

49 D. T. Do, S. D. Mahanti and J. Pulikkotil, *arXiv:1312.2985v1 [cond-mat.mes-hall]* 10 Dec 2013.

50 P. Blaha, K. Schwarz, G. K. H. Madsen, D. Kvasnicka, J. Luitz and K. Schwarz, *An Augmented Plane Wave plus Local Orbitals Program for Calculating Crystal Properties. Wien2K Users Guide, Wien* Techn. Universitat Austria (2008)

51 J. P. Perdew, K. Burke and M. Ernzerhof, *Phy. Rev. Lett.* 1996 **77** 3865-3868.

52 F. Tran and P. Blaha, *Phys. Rev. Lett.* 2009, **102**, 226401.

53 D. P. Rai, A. Shankar, Sandeep, M. P. Ghimire and R. K. Thapa, *Comput. Mater. Sci.* 2015, **101** 313320.

54 N.A. Zarkevich, T.L. Tan, D.D. Johnson, *Phys. Rev. B* 2007 **75** 104203.

55 A. Yakoubi, O. Baraka and B. Bouhafs, *Results in Physics* 2012, **2** 58-65.

56 Z. H. Zeng, F. Calle-Vallejo, M. B. Mogensen and J. Rossmeisl, *Phys. Chem. Chem. Phys.*, 2013, **15**, 7526.

57 F. D. Murnaghan, *Proc. Natl. Acad. Sci. USA* 1944, **30**, 244.

58 G. K. H. Madsen, and D.J. Singh, *Comput. Phys. Commun.* 2006, **175**, 67.

59 A. Slebarski, A. Jezierski, S. Lutkehoff and M. Neumann, *Phys. Rev. B* 1998, **57**, 6408.

60 R. M. Neiminen, *Topics in applied Physics: Theory of defects in semiconductors, Suoercell Methods for Defect Calculation* Vol. 104, edited by D. A. Drabold and S. K. Estreicher pp. 36-40 Springer (2006).

61 J. Heyd, G. E. Scuseria and M. Ernzerhof, *J. Chem. Phys.* 2003, **118**, 8207.

62 H. M. A. Yamamoto and T. Takeuchi *J. Appl. Phys.* 2014 **115** 023708.

63 T. Takeuchi *Mater. Trans.* 2009 **50** 2359.

64 G. D. Mahan Proc. *Natl. Acad. Sci. U.S.A* 1996 **93** 7436.

65 T. J. Scheidementel, C. A. Draxl, T. Thoonhauser, J. V. Badding and J. Sofo *Phys. Rev. B* 2003 **68** 125210.

66 K. Galazka, S. Populoh, W. Xie, S. Yoon, G. Saucke, J. Hulliger and A. Weidenkaff *J. Appl. Phys.* 2014, **115**, 183704.

67 S. Sakurada, N. Shutoh, *Appl. Phys. Lett.* 2005, **86**, 2105.

68 C. Yu. T. J. Zhu, R. Z. Shi, Y. Zhang, X. B. Zhao and J. He *Acta Mater* 2009, **57**, 2757.